To the Graduate Council:

I am submitting herewith a thesis written by Rodney Charles Wadley entitled "The Development and Characterization of a Macrocyclic Polyaminocarboxylic Acid and Its Metal Complexes As Potential Nuclear Magnetic Resonance Imaging Agents". I have examined the final copy of this thesis for form and content and recommend that it be accepted in partial fulfillment of the requirements for the degree of Master of Science, with a major in Chemistry.

Clifton Woods, III

Clifton Woods, III, Major Professor

We have read this thesis and recommend its acceptance:

James R. Chambers

William T. Bull

Accepted by the Council:

Lew Minkel

Associate Vice Chancellor
and Dean of The Graduate School

STATEMENT OF PERMISSION TO USE

In presenting this thesis in partial fulfillment of the requirements for a Master of Science degree at The University of Tennessee, Knoxville, I agree that the Library shall make it available to borrowers under rules of the Library. Brief quotations from thesis are available without special permission, provided that accurate acknowledgement of the source is made.

Permission for extensive quotation from or reproduction of this thesis may be granted by my major professor, or in his absence, by the Head of Interlibrary Services when, in the opinion of either, the proposed use of the material is for scholarly purposes. Any copying or use of the material in this thesis for financial gain shall not be allowed without my written permission.

Signature Rodney C. Wadley

Date July 25, 1991

THE DEVELOPMENT AND CHARACTERIZATION OF A MACROCYCLIC POLYAMINOCARBOXYLIC ACID AND ITS METAL COMPLEXES AS POTENTIAL NUCLEAR MAGNETIC RESONANCE IMAGING AGENTS

A Thesis

Presented for the

Master of Science Degree

The University of Tennessee, Knoxville

Rodney Charles Wadley

August 1991

DEDICATION

The author dedicates this work to his roommate and friend, Mr. Brian S. Haynesworth for his unyielding support and patience. A special dedication goes to his *Lord and Savior Jesus Christ* for giving him the intellectual ability to pursue higher educational goals.

ACKNOWLEDGEMENTS

The author wishes to thank Mr. Jinlong Cheng for helping him obtain T_1 relaxation times and he also would like to thank Dr. Woods for helping him finish his work in an expedient manner. A special thanks goes to Drs. George Kabalka and George Schweitzer for lending guidance in obtaining background literature.

A special thanks goes to his mother, Mrs. Burnette E. Edwards and his grandmother, Mrs. Ozie Dudley for giving him the confidence to believe in himself. Special gratitude is extended to Mr. and Mrs. Clarence Patrick and their lovely daughter, Nancy Eileen for their unselfish love and support over the past four years. Finally, the author would like to thank Joann Hickson for typing this thesis.

ABSTRACT

Diethylenetriaminepentaacetatogadolinium(III) [Gd(III)DTPA] is currently undergoing clinical trials as a magnetic resonance imaging (MRI) agent due to its remarkably high stability in-vitro and because of its high relaxivity (R_1) value. The goal of this research was to synthesize and characterize a new macrocyclic polyaminocarboxylic acid whose Fe(III), Gd(III), and Mn(II) complexes would exhibit comparable stabilities in-vitro as well as comparable R_1 values to the diethylenetriamine pentaacetic acid (DTPA) analogues. By obtaining and comparing the R_1 values of metal complexes of 1,4,7,10,13,16-hexaazacyclooctadecane-N,N′,N″,N‴,N⁗,N⁗′ -hexaacetic acid(OHA) with those of the DTPA analogues, this research qualifies the excellent potential of metal OHA complexes to be effective clinically as MRI agents.

TABLE OF CONTENTS

CHAPTER		PAGE
I.	Basic Introduction of NMR Imaging	
	A. Introduction	1
	B. Basic Theory of NMR	3
	1. Proton Magnetic Properties	3
	2. Resonance Phenomenon	5
	3. Proton Relaxation Times	8
	4. Inversion Recovery Method	11
II.	Complexes Used As MRI Agents	14
	A. Introduction	14
	B. Paramagnetic Contrast Agents	14
III.	Relaxivity of Metal Complexes	18
	A. Contributions to Relaxivity	18
	B. Statement of the Problem	20
IV.	Results and Discussion	21
	A. Synthesis of OHA	21
	B. Synthesis of Cu(II), Mn(II), Fe(III), and Gd(III) OHA	23
	C. Examination of Dicopper(II)OHA Magnetic Moments	23
	D. Examination of IR spectra: OHA, Cu(II)OHA, and Gd(III)OHA	25
	E. Examination of UV spectra: Cu(II) and Fe(III) OHA	30

TABLE OF CONTENTS

(continued)

CHAPTER		PAGE
	F. Relaxivity Measurements: OHA and DTPA Complexes	31
	G. Conclusions	35
V.	Experimental Methods	36
	A. General	36
	B. Synthetic Procedures	39
	1. Preparation of OHA	39
	2. Preparation of Metal OHA and DTPA Complexes	40
	C. Evans NMR Method: Magnetic Moment Calculations	41
	D. Inversion Recovery Method: Determination of T_1	42
	E. Relaxivity Calculations	44
List of References		45
Vita		48

LIST OF FIGURES

FIGURE PAGE

Figure 1. MRI of the brain. 2

Figure 2. The variation of T_1 and T_2 with correlation time, τ_c 12

Figure 3. Variable temperature ^1H NMR Spectra of OHA in D_2O . 24

Figure 4. IR spectrum of OHA (Nujol mull) 26

Figure 5. IR spectrum of Cu(II)OHA (Nujol mull) 27

Figure 6. IR spectrum of Gd(III)OHA (Nujol mull) 28

Figure 7. NOTA (1,4,7-triazacyclononane-1,4,7-triacetic acid) 30

CHAPTER I

BASIC INTRODUCTION TO NMR IMAGING

A. Introduction

Since its initial application by Bloch and Parcell, the phenomenon of magnetic resonance has been used widely by chemist and biochemists in the study of both inorganic and isolated organic compounds.[1] In its simplest form, nuclear magnetic resonance (NMR) is the study of the properties of molecules containing magnetic nuclei by observing the magnetic fields at which they come into resonance with an applied field of definite frequency.[2] Although a basic discussion of the NMR phenomenon will be given later, it is initially important to note that magnetic resonance imaging (MRI) is possible only because of clever manipulation of the NMR experiment; hence, it is possible to generate images such as the one shown in Figure 1.

Human tissue is largely composed of water; it is the NMR properties of the protons in aqueous solutions which are important in MRI. Bloch first described the use of a ferric nitrate solution to enhance the relaxation rates of water protons.[3] Consequently, it is the enhanced relaxation rate of protons which is the origin of a MRI.

NMR imaging is a very powerful complement to computerized tomography (CT) and positron emission tomography (PET), but unlike these techniques it involves no toxic radiation sources. This makes MRI attractive to physicians as well as patients.[4]

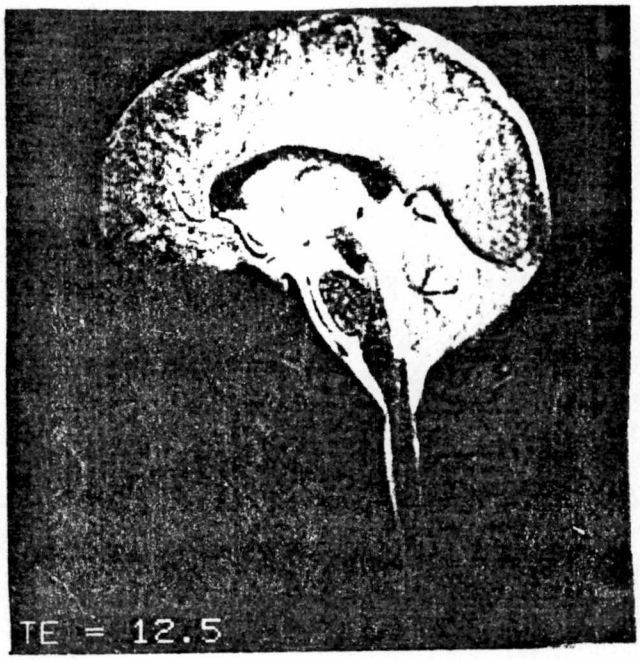

Figure 1. MRI of the brain.

[D. D. Stark, W. G. Bradley, Jr., et. al in

"Magnetic Resonance Imaging," C. V. Mosby Co., St. Louis, Missouri, 1982, p. 20]

B. Basic Theory of NMR

Although a rigorous discussion of the NMR theory is beyond the scope of this thesis, a basic understanding of the phenomenon is essential in appreciating MRI: only nuclei with spin can undergo the NMR phenomenon. Nuclei with spin contain either an odd number of protons, an odd number of neutrons or both; almost all elements have isotopes which have spin, represented by I, the net nuclear spin quantum number; nuclei with odd masses have I values which are multiples of 1/2, i.e. $I = n/2$ where $n = 1,2,3$, etc.; nuclei with even mass numbers and even atomic numbers have $I = 0$, no spin; nuclei with $I \geq 1$ have even mass numbers and odd atomic numbers, i.e. $I = 1,2,3$ ... etc. Since MRI is primarily associated with water solutions, attention will be focused on the hydrogen atom for which $I = 1/2$.

1. Proton Magnetic Properties

Since the proton possesses nuclear spin ($I = 1/2$) and a spherical nuclear charge, there is a nuclear magnetic moment (μ_N) and an angular momentum (J) associated with the nucleus. The magnetic moment and angular momentum vectors which arise as a result of the nucleus being placed into an applied external magnetic field, H_o are both oriented along the axis of rotation; orientations are defined by the magnetic nuclear spin quantum number, M_I, where $M_I = I, I-1, \ldots -I$. For the proton ($I = 1/2$) there are two possible orientations for M_I, $1/2$ and $-1/2$. $M_I = 1/2$ is defined as the low energy state and $M_I = -1/2$ is the high energy state.

The magnetic moment and angular momentum vectors are related by the equation

$$\mu_N = g_N(e/2m_pc)J \quad (1)$$

where g_N is the nuclear g-factor (a constant for a given nucleus), e is the electron charge, m_p is the proton rest mass, c is the speed of light, J is equal to

$$[I(I + 1)]^{1/2}\hbar \quad (2)$$

and $\hbar$ is $h/2\pi$; h is Plank's constant.

Equation 1 can be rewritten as

$$\mu_N = g_N (e/2m_pc) [I(I + 1)]^{1/2} \hbar$$

or

$$\mu_N = g_N(e\hbar/2m_pc)\hbar^{-1} [I(I + 1)]^{1/2}\hbar \quad (3)$$

where $e\hbar/2m_pc$ is B_N, the nuclear Bohr magneton.

Equation 3 is now written as

$$\mu_N = g_N B_N\hbar^{-1} [I (I + 1)]^{1/2}\hbar$$

or

$$\mu_N = g_N B_N\hbar^{-1} J. \quad (4)$$

When a nucleus is placed in a magnetic field, a torque, T, is generated which causes the magnetic moment vector to precess about the direction of the field at an angle θ as depicted on the following page.

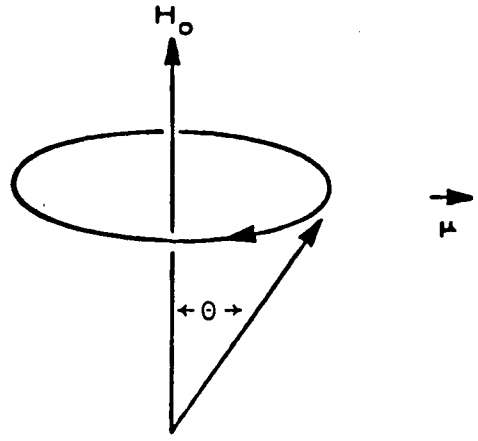

The torque is equal to the rate of change of the magnetic moment vector and is directly proportional to the strength of the magnetic field as described by the equation

$$T = \mu H_o = dJ/dt. \tag{5}$$

γH_o represents the frequency at which the magnetic moment precesses about the field direction. This frequency is called the Larmor frequency, ω_o, given by the equation

$$\omega_o = \gamma H_o \tag{6}$$

where γ is the gyromagnetic ratio given by

$$\gamma = g_N B_N h^{-1} = \mu_N/J. \tag{7}$$

2. Resonance Phenomenon

Resonance is defined as the induction of transitions from the $M_I = 1/2$ state to the $M_I = -1/2$ state for the proton. The energy required to produce such a transition is the difference in magnetic energy between the lower and upper states. Resonance occurs when radiofrequency (RF) energy is applied at the Larmor

frequency, flipping the magnetic moment vectors from their $M_I = 1/2$ (lower energy) to $M_I = -1/2$ (higher energy) states as illustrated below.

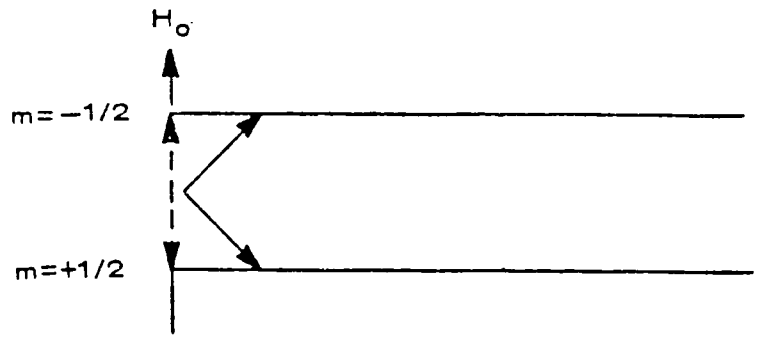

The energy difference between the two states is given by

$$E = (\mu_N/I)H_o. \tag{8}$$

For the proton, $I = 1/2$, the energy difference is the equivalent to $2\mu_N H_o$.

Since this energy difference is small compared to that of electronic energy states, the excited nuclear state may be highly populated at room temperature. The relative population of the states is given by the Boltzmann distribution

$$^*N/N = e^{-\Delta E/KT} \tag{9}$$

where N^* = Number of nuclei in the $M_I = -1/2$ state, N = Number of nuclei in the $M_I = 1/2$ state, K = Boltzmann constant, and T = Temperature (K). Equation 9 can be rewritten as

$$^*N/N = e^{-2\mu_N H_o/KT} \tag{10}$$

since $\Delta E = 2\mu_N H_o$. Even with an applied field of 14.09 KG, at room temperature, the excess population of the $M_I = -1/2$ state is very minuscule. As absorption of

resonant energy occurs, a dynamic equilibrium between the two energy states is established. In order to avoid saturation, the excited state nuclei must find a way to relax to the lower state. These relaxation mechanisms will be discussed later.

If a small radiofrequency (RF) field of amplitude H_1 is introduced perpendicular to the applied field H_o, at the Larmor frequency, resonance will occur, and the spins will "flip." Consider the magnetic moment vector precessing around H_o.

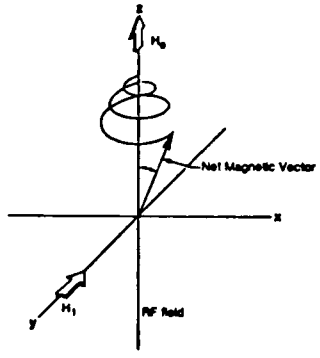

[A. Zermemo in "Nuclear Magnetic Resonance,"

R. C. Hichey, Ed., Yearbook Medical Publishers, Inc.,

Houston, Texas, 1982, p. 14]

When H_1 is applied along the y-axis, the magnetic vector tries to rotate about the y-axis or toward the x-axis. After the momentary application of H_1, the net magnetization is no longer aligned with the z-axis. Precession of the vector about H_1 now occurs at a frequency ω_1 given by

$$\omega_1 = \gamma H_1. \tag{11}$$

Precession about H_1 is also given as the change in θ per unit time of application of H_1 if H_1 is applied as a pulse. The precessional frequency is now given as

$$\omega = \theta/t_p \tag{12}$$

where t_p is the duration of the pulse; t_p is also called the pulse width (PW). Substitution gives

$$\theta/t_p = \gamma H_1 \tag{13}$$

and

$$\theta = \gamma H_1 t_p. \tag{14}$$

We will focus on those values of t_p which produce 90^0 and 180^0 spin flips.

3. Proton Relaxation Times

The process by which the excited state components of the magnetization return to their ground states following a RF pulse is termed relaxation. The perpendicular components, M_x and M_y, return to their ground states via T_2 (spin-spin or transverse) relaxation; the magnetization along the z-axis, M_z, returns to its ground state via T_1 (spin-lattice or longitudinal) relaxation. Although both relaxation mechanisms will be discussed, it is the T_1 relaxation time which will be highlighted due to its relevance to MRI.

The spin-lattice (T_1) relaxation is the return of the M_z component to the thermal equilibrium value, M_o following excitation. This return to equilibrium is exponential and is described by the following equation.

$$dM_z/dt = (M_o - M_z)/T_1 \tag{15}$$

T_1 Curve

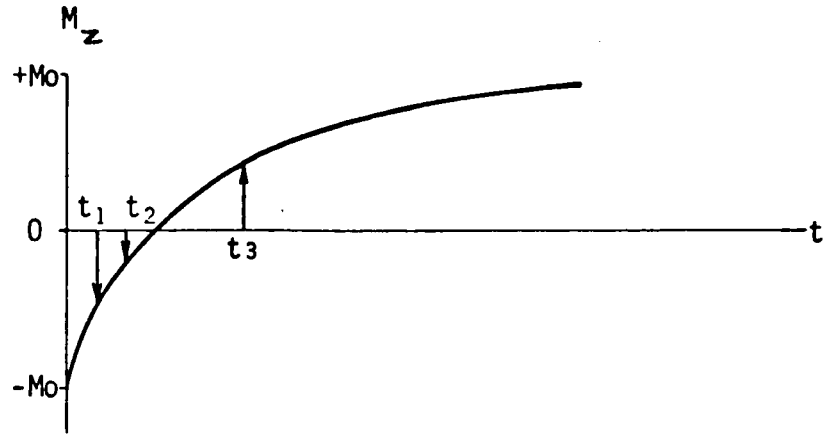

The return of M_z to equilibrium always involves the loss of energy from nuclei to the surroundings and is appropriately termed spin-lattice relaxation. The exchange of energy with the environment is the result of the interaction of the nucleus with fluctuating magnetic fields in the environment. The two major pathways which give rise to fluctuating magnetic fields are fields due to magnetic moments of other nuclei (intra- and inter-molecular) and fields associated with spins of unpaired electrons. The last pathway is the most significant contribution if paramagnetic species are present and will be discussed later.

The transverse (T_2) relaxation is the decay of the magnetization vector in the xy plane following excitation. This decay is also exponential and is expressed mathematically by the following equation.

$$dM_{xy}/dt = -M_{xy}/T_2 \qquad (16)$$

T_2 Curve

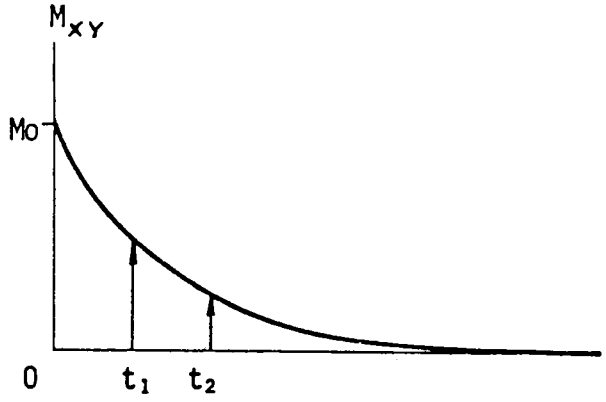

The M_{xy} vector is made up of the M_x and M_y components. The decay of M_{xy} is the result of the dephasing of the M_x and M_y components. This decay is an entropy-driven process and occurs as a result of the exchange of spins of different nuclei; transverse relaxation is thus called spin-spin relaxation. Inhomogeneity of the applied field also dephases spins.

The magnitudes of T_1 and T_2 can be associated with molecular motion. Rotational and translational motions are usually characterized by their correlation time, τ_c. The correlation time can be defined as the average time between collisions for translational motion and the average time for rotation by 1 radian for rotational motion. Correlation times depend on factors such as temperature, size of molecule, shape of molecule, and viscosity of the solution. Equation 17 gives the mathematical relationship for τ_c

$$\tau_c = 4\pi\eta a^3/KT \qquad (17)$$

where η is the solution viscosity and a is the radius of the molecule. The relationship between T_1, T_2, and τ_c is depicted in Figure 2.

4. Inversion Recovery Method

Since the T_1 (spin-lattice) relaxation time is the dominant factor in obtaining magnetic resonance images,[4] an efficient method for obtaining T_1 values is necessary. The inversion recovery method (IR), which is most commonly employed to obtain T_1, consists of a 180° RF pulse followed by a 90° RF pulse and is represented as $180° - \tau - 90°$.[5]

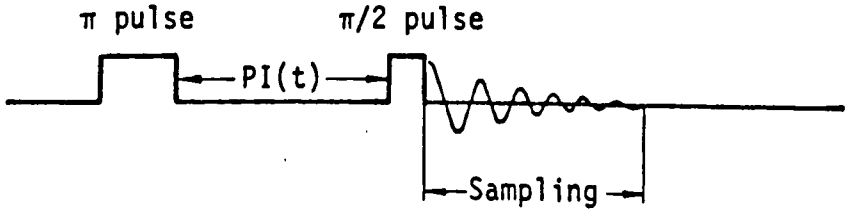

A 180° pulse is applied which flips the net magnetization, M_z 180°; after a time τ_1 (pulse interval or PI) a 90° pulse is applied which flips M_z along the y-axis where it is detected. A time greater than or equal to $5T_1$ (pulse delay or PD) between each pulse sequence is necessary to avoid saturation of the signal. Another 180° pulse is then applied and a PI of τ_2 is observed, where τ_2 is longer than τ_1. The longer τ_2 allows for more decay of M_z such that $M_z < M_o$. When the 90° pulse is now applied, the observed signal is less than the one observed after τ_1. If τ_3 is greater than τ_2,

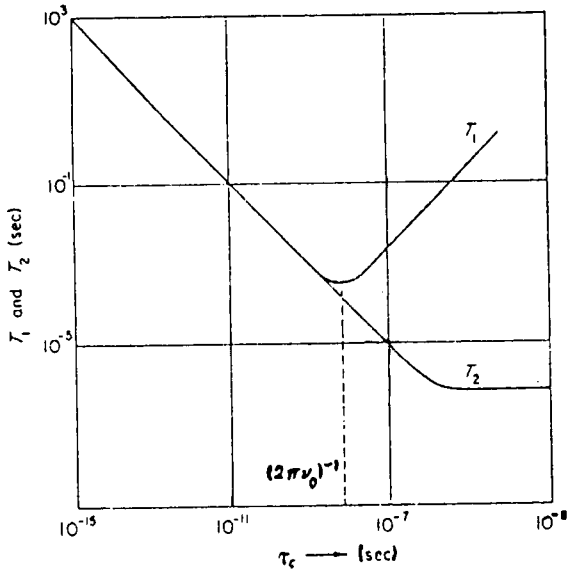

Figure 2. The variation of T_1 and T_2 with correlation time, τ_c.

[E. D. Becker in "High Resolution NMR: Theory and Applications,"

Academic Press, New York and London, 1972, p. 204]

the third signal is less than the second, and so on until a delay time τ_n is observed where no signal is obtained i.e. $M_z = 0$. For longer values of τ_n, the observed signal begins to increase. A plot of M_z versus τ is given as the T_1 curve on page 9. The value of M_z is given by

$$M_z = M_o\,(1-2e^{-\tau_n/T_1}). \tag{18}$$

τ_o, the value for which $M_z = 0$, is obtained experimentally and is given by the expression

$$\tau_o = T_1 \ln 2 \tag{19}$$

and

$$T_1 = \tau_o/0.693. \tag{20}$$

The relationship between MRI signal intensity (S), PI, and PD is given by the equation[5]

$$S = M_o(1-2e^{-PI/T1} + e^{-PD/T1}) \tag{21}$$

where M_o, the equilibrium value of the M_z magnetization, takes into account the proton density.

CHAPTER II

COMPLEXES USED AS MRI AGENTS

A. Introduction

The development of nuclear magnetic resonance imaging techniques as a clinical diagnostic modality has prompted the need for a new class of pharmaceuticals; these drugs would be administered to a patient in order to (1) enhance the image contrast between normal and diseased tissue and/or (2) indicate the status of organ function or blood flow.[4] As stated earlier, image intensity in ^{1}H NMR imaging is largely dependent on water proton nuclear relaxation times and to a lesser extent on proton density. Attempts to alter proton density by administration of lipid solutions, olive oil, and ethanol have been made with no significant change in signal intensity at safe dosages.[6] Attention has therefore focussed on paramagnetic species for image contrast enhancement.

B. Paramagnetic Contrast Agents

Paramagnetic ions contain unpaired electrons; if paramagnetic substances are present in solution, the magnetic moments from the unpaired electrons can furnish the basis for fluctuating magnetic fields.[7] The major difference is that the electron magnetic moment is approximately 1000 times that of the largest nuclear moment, so that relaxation by paramagnetic substances can be extremely effective. The relationship between T_1 and the magnetic moment of a paramagnetic molecule is given by the equation[7]

$$1/T_1 = 4\,\pi^2\gamma^2\eta N_p\mu^2_{eff}/KT \qquad (22)$$

where η = solution viscosity

N_p = concentration of paramagnetic species (mole/L)

μ^2_{eff} = the effective mean square magnetic moment of the ion

K = Boltzmann constant

and T = temperature (K)

Since T_1 is inversely proportional to the square of the magnetic moment and to the concentration of the paramagnetic species, the relaxation rate can be increased by increasing the concentration of the ion or by utilizing an ion with a larger magnetic moment.

Equation 22 also takes into account the correlation time, τ_c, as seen from equation 17; as stated earlier, Figure 2 graphically depicts the relationship between T_1 and τ_c. Hence, a possible approach to altering relaxation rates is to alter the correlation time.

Nitroxide stable free radicals (NSFR) are paramagnetic species having one unpaired electron localized in a nitrogen-oxygen bond. They have been developed and used as paramagnetic probes in biological studies for over 20 years.[8] The two major classes of nitroxides tested for MRI are the five-membered ring pyrolidine nitroxide 1 and the six-membered ring piperidine nitroxide 2. Nitroxide compounds have shown to be readily reduced in-vivo thus limiting their use as MRI contrast agents.[9,10]

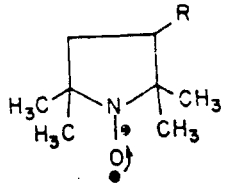

1

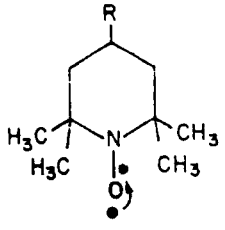

2

A second and more important class of paramagnetic species consists of metal ions of the transition metals and lanthanides. First row transition metal ions contain partially filled 3d orbitals. By virtue of Hund's rule, the five degenerate 3d orbitals are filled so as to give a maximum spin angular momentum. As a result, the metal ions Mn^{2+} and Fe^{3+}, have 5 unpaired electrons each and are very promising MRI contrast agents due to their large magnetic moments (5.9 Bohr magnetons). Metal ions of the lanthanide series with partially filled 4f orbitals are also strong possibilities. Gd^{3+} and Eu^{2+} with seven 4f electrons each and magnetic moments of around 7.9 Bohr magnetons are excellent candidates as MRI contrast agents.

Free metal ions, however, remain too toxic to be utilized as safe contrast agents;[11] therefore, attention has been focused on chelates which may bind metal

ions strongly enough to render them virtually non-toxic at effective levels. The polyaminocarboxylic acids ethylenediaminetetraacetic acid (EDTA) 3 and diethylenetriaminepentaacetic acid (DTPA) 4 with six and eight chelating sites, respectively, have received the most attention as ligands whose metal complexes are much less toxic than the respective free metal ions.

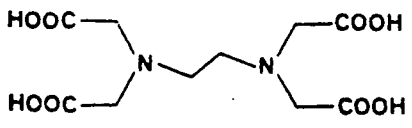

3

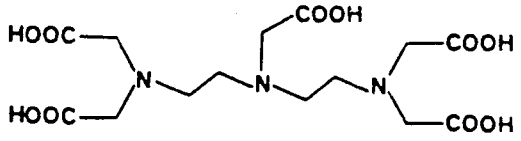

4

Gd(III)DTPA is the most attractive agent at present and currently is the only agent undergoing clinical trials;[4] the formation constant (log K) is 22.[12] Since Gadolinium(III) has a coordination number of 9 or 10, at least one site is open for rapidly exchanging water molecules. The availability of open coordination sites influences the complexes overall relaxation efficiency in solution as shall be discussed in Chapter III.

CHAPTER III

RELAXIVITY OF METAL COMPLEXES

A. Contributions to Relaxivity

The following summary emphasizes important features relevant to the relaxivity of metal complexes, a subject which has not received sufficient attention.[4]

Introduction of a paramagnetic complex into a solvent decreases T_1 and T_2, and so increases $1/T_1$ and $1/T_2$. Although the diamagnetic contribution to relaxation is usually small, the diamagnetic and paramagnetic contributions to the T_1 relaxation rate are additive and given by the equation

$$(1/T_1)_{OBSD} = (1/T_1)_d + (1/T_1)_p \tag{23}$$

where $(1/T_1)_{OBSD}$ is the observed solvent relaxation rate in the presence of a paramagnetic species, $(1/T_1)_d$ is the diamagnetic solvent relaxation rate in the absence of a paramagnetic species, and $(1/T_1)_p$ is the paramagnetic contribution to relaxation.

In the absence of solute-solute interactions, the solvent relaxation times are linearly dependent on the concentration ([M]) of the paramagnetic species. The relationship for this is given as

$$(1/T_1)_{OBSD} = (1/T_1)_d + R_1\,[M] \tag{24}$$

where R_1, the relaxivity, is defined as the slope of this dependence in units of $M^{-1}s^{-1}$ or, more commonly, $mM^{-1}s^{-1}$. R_1 values are very useful in comparing the relative T_1 reducing ability of paramagnetic metal complexes and shall be thoroughly

examined in the experimental section of this thesis.

The large and fluctuating local magnetic field in the vicinity of a paramagnetic center provides the largest relaxation pathway for solvent nuclei. Since these fields fall off rapidly with distance, random translational diffusion of solvent molecules and the complex as well as specific chemical interactions that bring the solvent molecules near the metal ion (e.g., within 5Å) are important in transmitting the paramagnetic effect.[4]

For the water proton, three distinct types of interactions are possible. In case **A**, a water molecule binds directly to the metal. In case **B** water molecules are hydrogen-bonded to the metal with some polar atom acting as a bridge. And in case **C** water molecules and the metal center are diffusing swiftly past each other (translational diffusion).

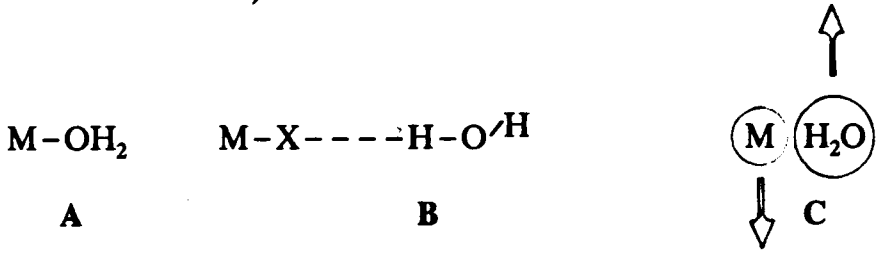

The mechanism for relaxation resulting from the interaction in case **A** is usually referred to as "inner-sphere relaxation." The interactions is cases **B** and **C** collectively result in what is termed "outer-sphere relaxation", since the second coordination sphere is not well understood. The total relaxivity of a paramagnetic agent is therefore generally given by

$$(1/T_1)_p = (1/T_1)_{\text{inner sphere}} + (1/T_1)_{\text{outer sphere}} \quad (25)$$

Complexes which have a large inner sphere contribution to relaxivity (i.e. water

molecules directly coordinated to the metal) usually have shorter T_1 times than comparable complexes which do not have inner sphere waters; this is very important in the design of potential MRI agents.

B. Statement of the Problem

Since Gd(III)DTPA is the only complex currently undergoing clinical trials as a MRI agent, it has been thoroughly reviewed and exhibits several very important characteristics: (1) it has remarkable stability in-vitro; log K is around 22[12] (2) it possesses at least one inner sphere water molecule and (3) Gd(III) has a very large magnetic moment independent of the ligand field.[13] Factors two and three lend to a very high R_1 value which as stated earlier is a very good indicator of relative T_1 reducing ability.

The purpose of this research was to synthesize and characterize a ligand whose metal complexes would be more stable or as stable as the DTPA analogues. In addition, our goal was to determine and compare R_1 values of these new complexes with the DTPA analogues. By pursuing the previously mentioned objectives in this research, we have examined the potential of a novel series of metal complexes as MRI agents.

CHAPTER IV

RESULTS AND DISCUSSION

A. Synthesis of OHA

One of the major objectives of this research was to synthesize a macrocyclic polyaminocarboxylic acid whose metal complexes would exhibit stability constants comparable to those of metal DTPA complexes. After several unsuccessful attempts to synthesize 1,4,10,13,16,22-hexaaza-7,19-dioxacyclotetracosane-N,N′,N″,N‴,N⁗,N⁗′ –hexaacetic acid 5, a ligand which would theoretically

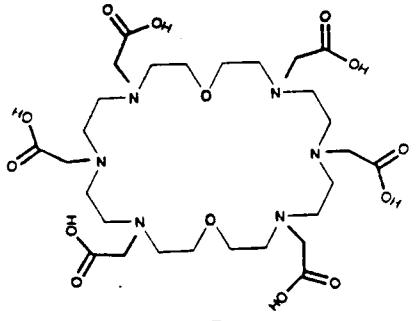

5

coordinate two Gd(III) ions and exhibit high stability in-vitro, attention was focussed on synthesizing 1,4,7,10,13,16-hexaazacyclooctadecane-N,N′,N″,N‴,N⁗,N⁗′-hexaacetic acid (OHA) 6 from 1,4,7,10,13,16-hexaazacyclooctadecane, 7.

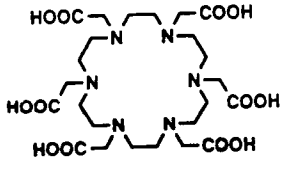

6

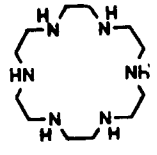

7

Since this new ligand would be macrocyclic, it was theorized that the "macrocyclic effect" would be operative and allow for appreciable thermodynamic and kinetic stabilities of metal complexes.

Coincidentally, the synthesis of this ligand along with thermodynamic and kinetic studies of its lanthanide complexes was reported by Kodama, et. al[16] during the course of this research. Although metal-ligand formation rates were found to be 10 times slower than those for DTPA, stability constants were found to be generally greater for OHA complexes; log K for Gd(III)OHA was found to be 22.95 versus 22.5 for Gd(III) DTPA at 25 °C.[16] These results provided excellent support for the necessity of carrying out relaxivity studies of OHA complexes.

The procedure employed for the synthesis of OHA was a modified version of that of Snyder.[14] The Hexaazacyclodecane, 7, was allowed to react with 6 equivalents of bromoacetic acid (BrOAc) under basic conditions to give OHA.

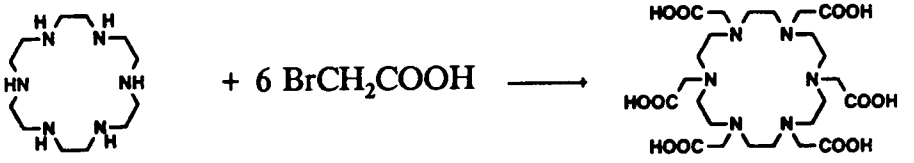

(26)

The cream-colored polyaminocarboxylic acid was isolated as the trihydrobromide trihydrate salt and was characterized by ^{1}H NMR spectroscopy, IR spectroscopy and elemental analysis. Variable temperature ^{1}H NMR was necessary to resolve the acetate and ethylenic protons due to the prevalence of peak overlappings at room temperature. With an increase in temperature, the acetate protons coalesce into a

sharp singlet around 4.064 ppm and the ethylenic protons coalesce into a second sharp singlet around 3.799 ppm, as illustrated in Figure 3d.

B. Synthesis of Cu(II), Mn(II), Fe(III), and Gd(III) OHA

Since copper(II) commonly forms complexes with coordination numbers less than six,[17] it was assumed that OHA which has twelve coordination sites would tend to form a dimeric species with copper. Therefore, $CuCl_2 \cdot 2H_2O$ was treated with one-half equivalent of OHA to form dicopper(II)OHA complexes. Mn(II), Fe(III), and Gd(III) were all expected to form monomeric complexes with OHA, therefore 1:1 ligand to metal ratios were used to synthesize these complexes. In most cases, the pH was adjusted to about 7 and temperatures were elevated during complexation to prevent formation of metal hydroxides. Dicopper(II)OHA complexes were vivid sky-blue in color; Fe(III)OHA solutions were yellow; Mn(II)OHA and Gd(III)OHA solution were colorless; solid Gd(III)OHA was a cream-colored crystalline material.

C. Examination of Dicopper(II)OHA Magnetic Moments

Dicopper(II)OHA solutions were prepared in two different ways in order to examine how pH influences the magnetic interaction between Cu(II) atoms; magnetic moments were taken for an acidic (pH 2.0) solution of dicopper(II)OHA and for a solution with pH around 7.0 utilizing the Evans ^1H NMR method.[15]

For the solution with acidic pH, an effective magnetic moment of 2.06 Bohr magnetons was calculated which indicates that there is no interaction between metal atoms. Each Cu(II) ion behaves as a single monomeric unit.

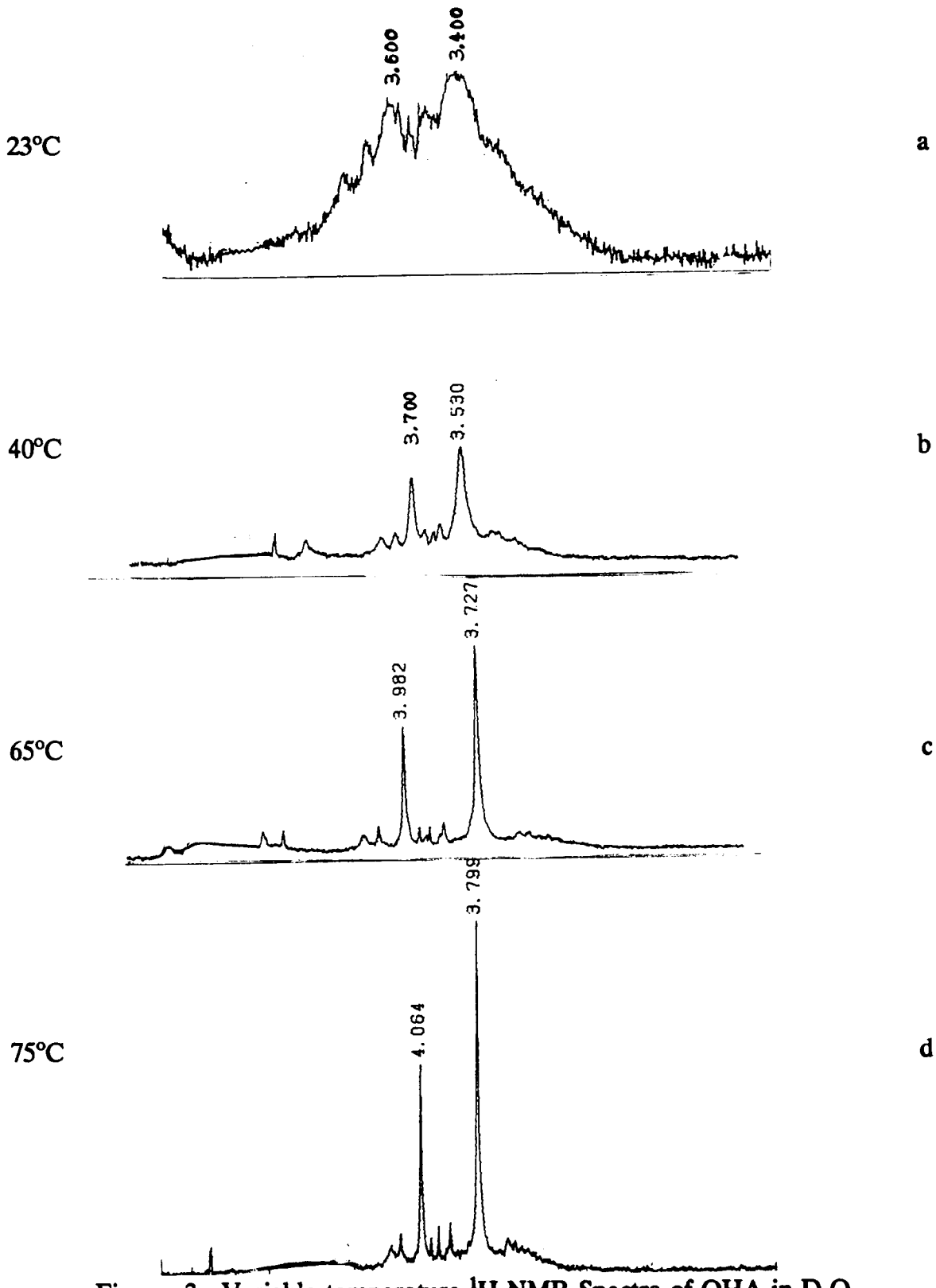

Figure 3. Variable temperature ^1H NMR Spectra of OHA in D_2O

For the solution with neutral pH, an effective magnetic moment of 1.65 Bohr magnetons was reported which indicates a slight antiferromagnetic exchange between the unpaired electron of each metal center. This interaction may be due to carboxylato bridging and/or hydroxo bridging. Since the magnetic moment remains relatively high for a dimeric species,[13] it is speculated that the triplet state associated with a Cu(II) dimer is appreciably populated with respect to the singlet state at room temperature.

D. Examination of IR spectra: OHA, Cu(II)OHA and Gd(III)OHA

Since NMR spectroscopy could not be utilized on the various metal OHA complexes due to paramagnetic broadening, the only spectroscopic method employed for their characterization was infrared (IR). For both Cu(II)OHA and Gd(III)OHA a drastic change occurred in the carbonyl region (1500 – 1800 cm^{-1}) as compared to the corresponding carbonyl region of the free ligand. These changes are illustrated in the IR spectra of OHA, Cu(II)OHA, and Gd(III)OHA as shown in Figures 4, 5, and 6, respectively. This phenomenon can be explained in the following manner. To an excellent approximation, the vibrational frequency of a bond is related to the masses of the vibrating atoms and to the force constant of the bond. Equation 27

$$\nu \propto [k/4\pi^2\mu]^{1/2} \tag{27}$$

states that the vibrational frequency of a bond is directly proportional to the square root of the force constant (k) and is inversely proportional to the square root of the

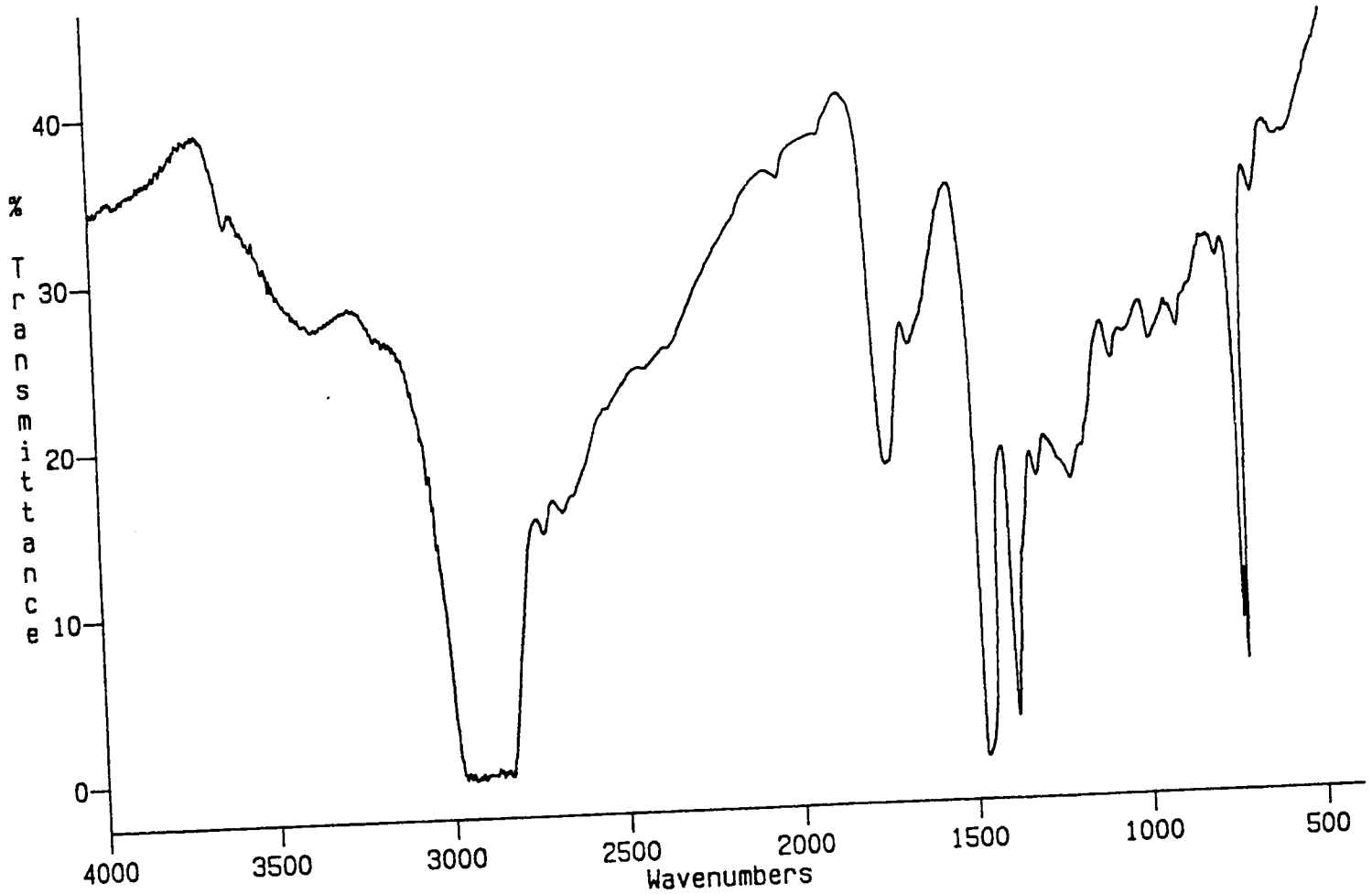

Figure 4. IR spectrum of OHA (Nujol mull)

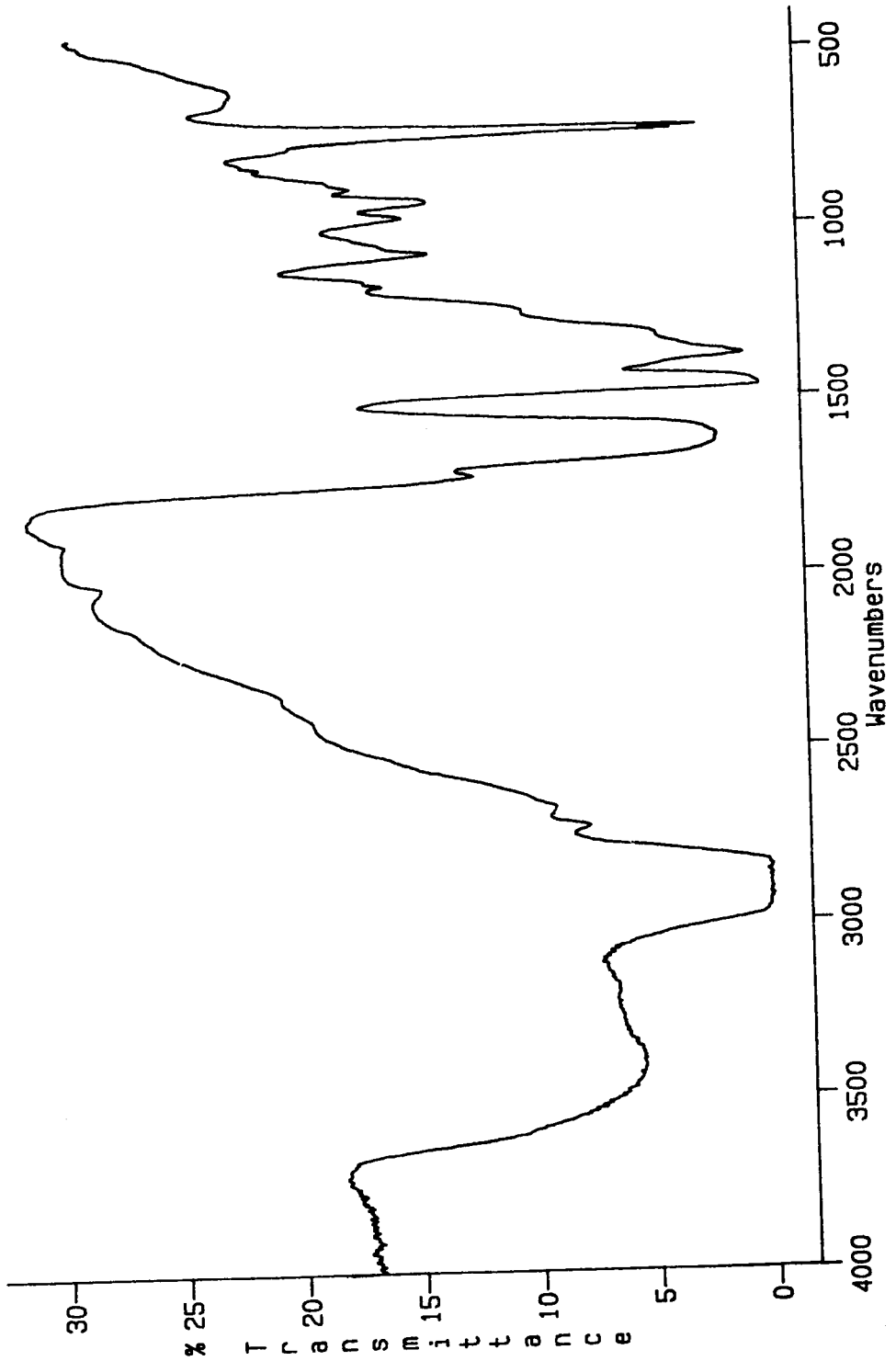

Figure 5. IR spectrum of Cu(II)OHA (Nujol mull)

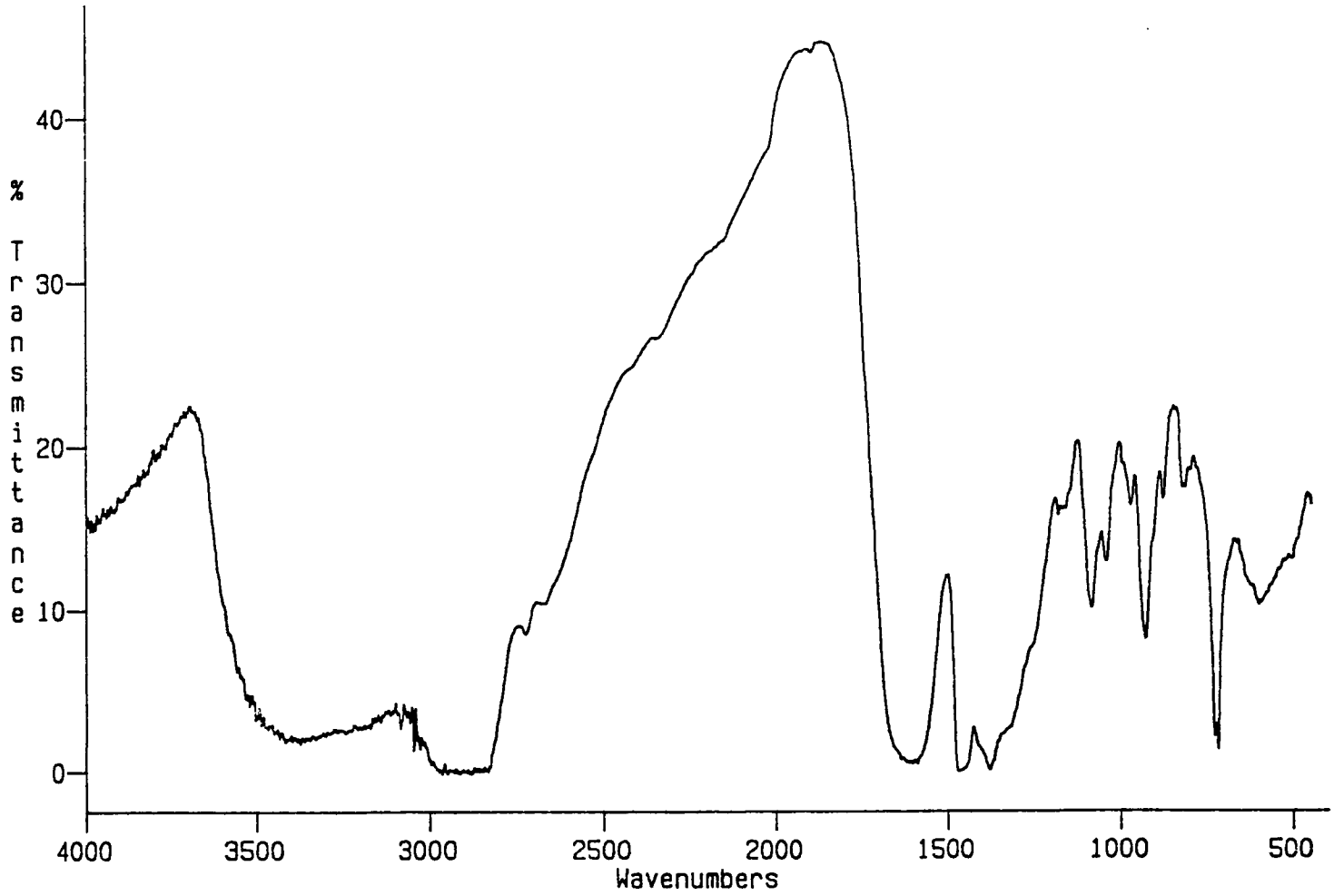

Figure 6. IR spectrum of Gd(III)OHA (Nujol mull)

reduced mass (μ) of the bond. Since the force constant is directly proportional to the bond order, the magnitude of the vibrational frequency is directly related to the bond order. The absorption for a carbon-carbon triple bond therefore occurs at a higher wavenumber than that for a carbon-carbon double bond.

In the study involving the complexation of various metals with EDTA, it was observed that the absorption band of the carbonyl bond in the unionized uncoordinated carboxylic acid group occurred at 1700–1750 cm^{-1} whereas the absorption band of the carbonyl bond in an ionized, coordinated carboxylate group occurred at 1590–1650 cm^{-1}.[18] The observed shift to lower energy was attributed to metal complexation in which both oxygen atoms of the carboxylate are involved in complexation. Bond order is therefore decreased from 2 to 1.5.

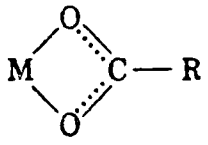

Based on the previous observations, the IR spectra of OHA, Cu(II)OHA, and Gd(III)OHA can be interpreted. In the IR spectrum of OHA (Fig. 4), the major absorption occurs at 1738 cm^{-1} which corresponds to the carbonyl bonds of the carboxylic acid groups which are connected to amine nitrogens. The smaller absorption band occurring at 1662 cm^{-1} which corresponds to a deprotonated group indicates that the species probably exists as a zwitterion. In the IR spectrum of

Cu(II)OHA and Gd(III)OHA (Figures 5 (p.27) and 6 (p. 28) respectively), the major absorption bands now occur at 1624 cm^{-1} and 1617 cm^{-1}, respectively. These shifts to lower energy presumably occur as a result of the previously illustrated metal complexation interaction. Thus, IR spectra are good indicators that complexation has occurred in metal OHA complexes.

E. Examination of UV Spectra: Cu(II) and Fe(III) OHA

To determine the relative strength of the ligand field produced by metal complexation with OHA, ultraviolet-visible spectra were taken for Cu(II) and Fe(III) OHA. The major absorbances which correspond to a metal d-d transition for the Cu(II) complex and a ligand to metal charge-transfer for the Fe(III) complex, were compared with those of the Cu(II) and Fe(III) NOTA (Figure 7) analogues at neutral pH and 25 °C.[19]

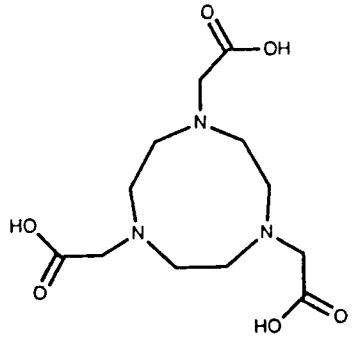

Figure 7. NOTA (1,4,7-triazacyclononane-1,4,7-triacetic acid)

As seen in Table 1, all λ_{max} values are lower for OHA complexes as compared to the NOTA complexes. Since lower wavelengths correspond to higher energies, it

can be concluded that the ligand field strength is greater in the presence of OHA as compared to NOTA.

Molar extinction coefficients which indicate the relative probability of a transition occurring are also listed in Table 1.

Table 1

UV–Visible Data

Complex	λ_{max},nm(ϵ,L mol^{-1}cm^{-1})
Fe(III)NOTA	257(1.2×10^4)
Cu(II)NOTA	750(72.2)
Fe(III)OHA	244(6.6×10^3)
Cu(II)OHA	728(45.1)

In all cases, the molar extinction coefficients (ϵ) of the OHA complexes are less than those for the NOTA analogues.

F. Relaxivity Measurements: OHA and DTPA Complexes

Relaxivity (R_1) values were calculated by obtaining the least-squares slope of the line generated by plotting $(1/T_1)_{OBSD}$ against concentration (mM) for DTPA as well as OHA complexes and is illustrated in Chapter V section E. Relaxivity (R_1) values at 22 °C are listed in Table 2 for important OHA and DTPA complexes.

Table 2

Relaxivity (R_1) Values for OHA and DTPA Complexes

Complex	$R_1(mM \cdot sec)^{-1}$ 22°C
Fe(III)OHA	0.48
Mn(II)OHA	4.4
Mn(II)DTPA	0.75
Gd(III)OHA	8.2
Gd(III)DTPA	4.6

In all cases, the OHA complexes exhibit greater relaxivity (R_1) values than their DTPA analogues. These results warrant a thorough explanation which is given in the subsequent paragraphs.

Since Mn(II)DTPA is known to have zero inner sphere water molecules,[4] the outer sphere contribution to relaxivity must be important. Although Mn(II)OHA should also be expected to have zero inner sphere water molecules due to OHA's twelve chelating sites, the outer sphere contribution to relaxivity should be greatly enhanced due to the increased availability of free carboxylate and amine groups which can hydrogen bond water molecules as depicted on the following page. Another factor which affects R_1 as a consequence of affecting T_1 is the correlation

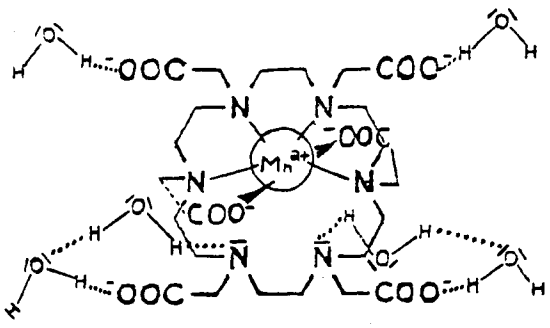

time, τ_c. Since it can be logically assumed that the overall molecular radius(a) of OHA complexes will be greater than the radius of analogous DTPA complexes, τ_c should increase as suggested by Equation 17

$$\tau_c = 4\pi\eta a^3/KT \qquad (17)$$

assuming that all other variables remain constant. Since τ_c increases, T_1 should decrease as illustrated by Figure 2, p. 12; the major assumption here is that the correlation times we are dealing with are to the left of the curve minimum, the area which is associated with small molecules and small metal complexes.[7] Furthermore, the expected increase in correlation time, τ_c, in conjunction with the enhanced contribution to outer sphere relaxivity increases the R_1 value of Mn(II)OHA over the value for Mn(II)DTPA.

A similar argument can be presented for the increased R_1 value of Gd(III)OHA as compared to the value for Gd(III)DTPA. Since Gd(III)DTPA is expected to have at least one inner sphere water molecule,[4] the inner sphere contribution of relaxivity must be dominant as explained in Chapter III section A, p. 18. Although we could not determine the exact number of inner sphere water molecules that Gd(III)OHA possesses, it is assumed that the Gd(III) ion is coordinatively saturated and has zero

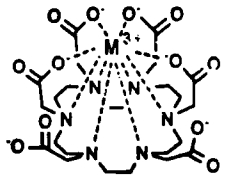

M = Gd^{3+}

inner sphere water molecules as depicted above. As explained in the case of Mn(II)OHA, Gd(III)OHA should exhibit a considerable outer sphere mechanism to relaxation provided by hydrogen bonding. Large τ_c values are generally accompanied by small T_1 values for a given complex. Since Gd(III)OHA is expected to have a τ_c value greater than that of Gd(III)DTPA, the T_1 values for Gd(III)OHA are expected to be smaller than those for Gd(III)DTPA. Although Gd(III)OHA probably contains no inner sphere water molecule, the greater correlation time and the enhanced outer sphere contribution to relaxivity combine to increase the overall R_1 value of the complex in comparison to the R_1 value for the DTPA analogue.

Fe(III)OHA, on the other hand, is an anomaly. Since aqueous solutions of Mn(II) and Fe(III) have identical magnetic moments, it was assumed that the corresponding OHA complexes would exhibit similar R_1 values. As seen in Table 2, this is definitely not the case; the R_1 value of Fe(III)OHA is approximately one order of magnitude less than the value for Mn(II)OHA and is less than the value for Mn(II)DTPA as well. The low R_1 value of Fe(III)OHA is probably a consequence of Fe(III)'s tendency to form hydroxo-complexes even at neutral pH;[13] such

complexes would decrease the assessability of the Fe(III) ion to water molecules and would decrease the relaxing efficiency of the ion.

G. Conclusions

The polyaminocarboxylic acid, OHA, has been synthesized and characterized along with selected metal complexes. The work of Kodama, et. al[16] illustrated that most OHA lanthanide complexes are more stable in-vitro than the corresponding DTPA complexes. The relaxivity (R_1) measurements which we obtained have shown that Mn(II)OHA and Gd(III)OHA are more efficient at relaxing the spins of water protons than their DTPA analogues. Since in-vitro stability and efficient relaxivity are important prerequisites for an effective contrast agent,[4] these new complexes warrant further testing in clinical trials as MRI agents.

CHAPTER V

EXPERIMENTAL METHODS

A. General

All glassware was oven-dried prior to use. All infrared spectra were taken on a Biorad FTS-7 FT-IR spectrometer and are reported in cm^{-1}; all samples (ligand and metal complexes) were ground into nujol mulls and sealed between two thin sheets of polyethylene. All variable temperature ^1H NMR spectra were taken on a Nicolet 200 MHz FT-NMR spectrometer. The instrument was locked on the deuterium signal of D_2O (used as solvent); all chemical shifts are reported in ppm using tetramethylsilane (TMS) as an internal reference (δ = 0.0 ppm). All data for determinations of T_1 relaxation times were obtained on a Bruker AC 250E FT-NMR spectrometer using chloroform-d ($CDCl_3$), flame-sealed in a 4 mm tube, as an internal lock. Data for calculations of magnetic moments by the Evans NMR method were obtained on a Nicolet 200 MHz FT-NMR spectrometer. Ultraviolet-visible spectra were obtained with a HP 8452A Diode Array spectrometer. Quartz cells (Fisher Scientific) of 1.0 cm pathlength were used; distilled water was used as the solvent. Elemental analysis were provided by Galbraith Laboratories, Knoxville, Tennessee. All commercially obtained chemicals, their manufacturers and methods of purification, when applicable, are listed in Table 3.

Table 3

Sources and Purification Methods
of Commercially Available Chemicals

Chemical and Abbreviations	Source[a]	Purification Methods[b]
Ammonium Hydroxide (NH_3)	B	1
Bromoacetic Acid (BrOAc)	A	
Chloroform-d ($CDC1_3$)	C	
Copper Dichloride Dihydrate ($CuCl_2 \cdot 2H_2O$)		
Deuterium Oxide (D_2O)		
Diethylenetriamine-pentaacetic Acid (DTPA)	A	
Diethyl Ether	C	
Distilled Water	D	
Dowex-50×4-400 Ion-Exchange Resin	A	3
Ethanol (EthOH)	E	
Gadolinium Trichloride Hexahydrate ($GdCl_3 \cdot 6H_2O$)	A	
1,4,7,10,13,16-hexaazacyclooctadecane	A	
Hydrobromic Acid (HBr)	A	
Iron Trichloride Hexahydrate ($FeCl_3 \cdot 6H_2O$)	B	
Manganese Sulfate Monohydrate ($MnSO_4 \cdot H_2O$)	B	
Nujol	B	2
Sodium Hydroxide (NaOH)	C	
Sodium Metal (Na)	B	

Table 3

(continued)

Chemical and Abbreviations	Source[a]	Purification Methods[b]
Tetramethylsilane (TMS)	A	

[a]Sources

A = Aldrich
B = Fisher Scientific
C = Mallinckrodt
D = Departmental Still
E = Midwest Grain Products Company

[b]Purification Methods

1 = Dried under vacuum
2 = Dried over Na metal
3 = Washed with 50 ml 1 M HCl; then eluted with 100 ml distilled water

B. Synthetic Procedures

1. Preparation of 1,4,10,13,16,22-hexaaza-7,19-dioxacyclotetracosane-N,N′,N″,N‴,N⁗,N⁗′-hexaacetic acid (OHA)

OHA was prepared by the method of Synder and coworkers.[14] BrOAc (11.772 g, 0.083 moles) in a 50% excess and the cyclohexamine, 7, (5.098 g, 0.0092 moles) were neutralized separately with stoichiometric amounts of NaOH in 50 and 250 milliliters of distilled water, respectively; the temperature of the BrOAc solution was maintained around 0 °C during the neutralization reaction. The resulting solutions were combined with magnetic stirring and the temperature was raised to 60 °C; 6M NaOH (15.01 mL) was added over a 24 hour period to maintain a pH between 9 and 10. When the reaction ceased (when no further NaOH was required) enough HBr (48%) was added to bring the pH to around 2.0. The solution was then precipitated with EtOH, loaded onto a column of 46.0 g of Dowex 50 W-X4 (100-200 Mesh) cation exchange resin in the H^+ form, and eluted with 46 mL of distilled water (one column volume) followed by 0.50 M NH_3. A flow rate of about 2 mL/min was used and 20 mL fractions were collected. Anions (mostly Br^- and SO_4^{2-}) pass directly through the column; cations (mostly Na^+ from NaOH) adhere to the resin displacing H^+, and the desired product is displaced by the NH_3. Fractions containing the purified product had a pH between 2 and 5, and these were saved. Saved fractions were then combined and reduced in volume under water aspirator at 80 °C until crystals began to form. Addition of a volume of EtOH equal to 3 times the solution volume induced further precipitation. After filtering, the precipitate was washed with

EtOH and diethyl ether and dried under vacuum at 70 °C. Total yield was 2.50 g, 30.1%. ^{1}H NMR (200 MHz, D_2O, 40 °C): δ 3.70 (S, 12H, NCH_2COO), 3.53 (S, 24 H, NCH_2CH_2N); IR (Nujol): 3375 (br, O-H), 1738 (acid C=O), 1662 (carboxylate C=O); Elemental analysis: calculated for $C_{24}H_{42}N_6O_{12}\cdot 3HBr\cdot 3H_2O$; %C = 31.91, %H = 5.69, %N = 9.31. Found; %C = 32.61, %H = 5.62, %N = 8.61.

2. Preparation of Metal OHA and DTPA Complexes

Dicopper(II)OHA was prepared for IR spectroscopy by dissolving OHA (0.182 g, 0.00020 moles) and $CuCl_2\cdot 2H_2O$ (0.068, 0.00040 moles) in separate 25 mL aliquots of distilled water. The two solutions were then mixed while stirring and a vivid blue solution immediately resulted. The temperature of the solution was then elevated to 50 °C and 6 M NaOH was added dropwise to adjust the pH to around neutral. After approximately ten minutes equilibration time, the pH was checked again to assure that it remained around 7.0. Water was then removed by water aspiration to give about 10 mL of solution. EtOH was added to precipitate the complex which was filtered, washed with EtOH and diethyl ether, and dried in vacuo to give 0.150 g of a sky blue powder. IR (Nujol): 1624 (carboxylate C=O).

Gd(III)OHA was prepared for IR spectroscopy similarly, except that a 1:1 ratio of $GdCl_3\cdot 6H_2O$ to ligand was used; in addition, the reaction temperature was elevated to 90 °C to prevent the formation of Gd(III) hydroxide. A pale cream-colored crystalline solid was isolated. IR (Nujol): 1617 (carboxylate C=O). Millimolar solutions of Fe(III), Gd(III), and Mn(II) OHA complexes used for measuring T_1 relaxation times were prepared by dissolving the stoichiometrically

required amounts of metal salts and ligand (1:1 ratio) in 50 mL volumetric flasks. In each case, the temperature was elevated to 90 °C with stirring and the pH was raised to neutral with 6M NaOH. As before, ten minutes equilibration time was allowed and the pH was maintained around 7.0. The resulting solutions were allowed to cool to room temperature; 0.30, 0.50 and 0.70 mM solutions of each complex were then prepared by diluting appropriate amounts of the original solutions in 5 mL volumetric flasks. Mn(II) and Gd(III) DTPA solutions whose concentration were 0.30, 0.50 and 1.0 mM were used for T_1 measurements and were prepared in the same manner as those of the OHA complexes.

Two batches of dicopper(II)OHA used for magnetic moment calculations were prepared by identical procedures, except that the pH in batch #1 was left unadjusted and in the acidic range (approximately 2.0).

C. Evans NMR Method: Magnetic Moment Calculations

For each batch of dicopper(II)OHA (neutral or acidic) 5 mL of solution was added to a 10 mL volumetric flask while 5 mL of H_2O was added to a separate 10 mL flask. 1 mL of EtOH was then added to each flask followed by dilution to the mark with 4 mL of D_2O. The two solutions differed only by presence or absence of the paramagnetic species in one. By using the solution without the paramagnetic species as an internal reference, we then obtained the ^1H NMR spectrum to observe the difference in chemical shifts between two peaks (i.e. two H_2O peaks or two EtOH peaks) which in the absence of a paramagnetic species would have identical chemical

shifts. From equation 28 below[15] the effective magnetic moment of each copper(II) ion was calculated.

$$\mu_{eff} = 0.0618(\Delta f \cdot T/f \cdot [M])^{1/2} \quad (28)$$

Δf is the frequency (Hz) difference between the two peaks, T is the operating temperature (K), f is the ^1H resonance frequency in MHz, and [M] is the concentration of the paramagnetic species in units of mole/liter (M).

Sample calculation for dicopper(II)OHA under acidic conditions: Δf for the two H_2O peaks = 36.97 Hz, T = 297.15 K, f for ^1H resonance = 200 MHz, [M] = 1.25×10^{-2} M

$$\mu_{eff} = 0.0618(36.97\ Hz\times297.15K/200\ MHz\times1.25\times10^{-2}M)^{1/2}$$

$$\mu_{eff} = 4.1\ B.M. \quad (29)$$

$$\mu_{eff}/Cu(II)ion = 4.1\ B.\ M./2 = 2.1\ B.M./Cu(II)ion$$

D. Inversion Recovery Method: Determination of T_1

T_1's were measured at 22 °C using a Bruker AC 250E FT-NMR spectrometer operating at 250.068 MHz and a static field strength of 5.8719 Tesla. T_1's were determined by using the inversion recovery sequence (see pgs. 11 – 13). PD was set at 5.0 sec in all cases. Ten values of PI were used ranging from 0.00020 seconds to 2.50 seconds. The PIs were increased stepwise resulting in a curve of magnetization (M_z) recovery time similar to the one shown on page 9. T_1s were computed by the spectrometer computer on hand from a least-squares fit of the acquired exponential curve. T_1 values for the complexes at various concentrations are listed in Table 4.

Table 4

T_1 Relaxation Times

Complex	Concentration (mM)	T_1 (seconds)
Fe(III)OHA	0.30	0.687
Fe(III)OHA	0.50	0.664
Fe(III)OHA	1.0	0.563
Mn(II)OHA	0.30	0.162
Mn(II)OHA	0.50	0.191
Mn(II)OHA	0.70	0.238
Mn(II)OHA	1.0	0.322
Gd(III)OHA	0.30	0.272
Gd(III)OHA	0.50	0.223
Gd(III)OHA	0.70	0.163
Gd(III)OHA	1.0	0.108
Gd(III)DTPA	0.30	0.522
Gd(III)DTPA	0.50	0.361
Gd(III)DTPA	1.00	0.197
Mn(II)DTPA	0.30	0.469
Mn(II)DTPA	0.50	0.459
Mn(II)DTPA	1.0	0.380

E. Relaxivity Calculations

From Equation 24, p. 18, $(1/T_1)_{OBSD} = (1/T_1)_d + R_1[M]$ which has the form of the point-slope formula, $y = \beta x + \alpha$, we obtained R_1 values for each complex by plotting $(1/T_1)_{OBSD}$ against [M]. A least-squares fit of the data points using the following equations[20] allowed us to calculate a β value which theoretically is the R_1 value for a complex.

$$S_{xx} = \Sigma x_i^2 - (\Sigma x_i)^2/n \tag{29}$$

where n = number of data points, $y_i = (1/T_1)_{OBSD}$ and x_i = [M].

$$S_{xy} = \Sigma x_i y_i - \Sigma x_i \Sigma y_i/n \tag{30}$$

$$\bar{x} = \Sigma x_i/n \tag{31}$$

$$\bar{y} = \Sigma y_i/n \tag{32}$$

$$\beta = S_{xy}/S_{xx} \tag{33}$$

and

$$\alpha = \bar{y} - \beta\bar{x} \tag{34}$$

$(1/T_1)_d$, the diamagnetic contribution to relaxivity, is given as α, the y-intercept of the least-squares fit.

LIST OF REFERENCES

LIST OF REFERENCES

1. Foster, M. A. *Magnetic Resonance in Medicine and Biology*; Pergamon Press: Elmsfrod, New York, 1984, p. 1.
2. Atkins, P. W. *Physical Chemistry*; W. H. Freeman and Company: New York, 1986, p. 621.
3. Bloch, F.; Hansen, W. W.; Packard, M. *Phys. Rev.* **1948**, 70, 474.
4. Lauffer, R. B. *Chem. Reviews* **1987**, 87, 901–911.
5. Gore, J. C. *Nuclear Magnetic Resonance and Correlative Imaging Modalities*, C. L. Partain Ed., *The Society of Nuclear Medicine, Inc.*, New York, 1984, pp. 75–85.
6. Moss, T. M.; *MS Thesis*, University of Tennessee, Knoxville, 1986.
7. Becker, E. D. *High Resolution NMR*; Academic Press: New York and London, 1972, pp. 202–208.
8. Stone, T. J.; Buckman, T.; Nordio, P. L.; McConnell, H. M. *Proc. Nat. Acad. Sci. USA* **1965**, 54, 1010.
9. Couet, W. R.; Brasch, R. C.; Sasnovsky, G.; Tozer, T. N. *Magn. Reson. Imaging* **1985**, 3, 83–88.
10. Griffith, L. K.; Rosen, G. M.; Rauchman, E. J.; Drayer, B. P. *Invest. Radiol.* **1984**, 19, 553.
11. Kang, Y. S.; Gore, J. C. *Invest. Radiol.* **1984** 19, p. 408.

12. Martell, A. E.; Smith, R. M. *Critical Stability Constants*; Plenum: New York, 1989, p. 6.

13. Cotton, F. A.; Wilkinson, G. *Advanced Inorganic Chemistry*; John Wiley and Sons: New York, 1988, p. 717.

14. Snyder, J.; Synder, R. V.; Angelich, R. J. *Inor. Nucl. Chem.*, **1973**, 35, 524–525.

15. Evans, N. *J. Chem. Soc., Dalton Trans.* **1979**, p. 723.

16. Kodama, M.; Koike, T.; Mahatma, A. B.; Kimura, E. *Inorg. Chem.* **1991**, 30, 1270–1273.

17. Moi, M. K.; Yanuck, M.; Deshpande, S. V.; Hope, H.; DeNardo, S. J.; Meares, C. F. *Inorg. Chem.* **1987**, 26, 3458–3463.

18. Swaminathon, K.; Busch, D. H. *J. Inorg. Nucl. Chem.* **1961**, 20, 159.

19. Weighart, K.; Blossek, U.; Chaudhuri, P.; Herrman, W.; Menke, B. C.; Weiss, D. J. *Inorg. Chem.* **1982**, 21, 4308–4314.

20. Skoog, D. A.; *Principles of Instrumental Analysis*; Saunders College Publishing: Philadelphia, 1985, p. 20.

VITA

Rodney Charles Wadley was born on January 4, 1966 in Soperton, Georgia. He graduated from Treutlen County High School in 1984. Although he received an appointment to the United States Naval Academy, he attended Mercer University in Macon, Georgia where he received the B.A. degree in Chemistry in 1988. In August 1988 he entered the University of Tennessee and began graduate studies under the direction of Dr. Clifton Woods and received a Master of Science Degree in Chemistry in August 1991. He received a U.S. Army commission as a Distinguished Military Graduate in August 1989 and is now a clinical chemistry officer stationed in Fort Lewis, Washington.